Optimizing Training-Based Transmission Against Smart Jamming

Xiangyun Zhou, *Member, IEEE*, Dusit Niyato, *Member, IEEE*, and Are Hjørungnes, *Senior Member, IEEE*

***Abstract*—We consider training-based transmissions over multiple-input–multiple-output (MIMO) fading channels in the presence of jamming. Each transmission block consists of a training phase and a data transmission phase. From an information-theoretic viewpoint, we study the optimal energy allocation between the two phases for both the legitimate user of the channel and the jammer. For a fixed jamming strategy, we derive a closed-form solution of the optimal transmit energy allocation for the legitimate user and show that the optimal training length is equal to the number of transmit antennas. On the other hand, if the jammer has optimized its strategy, the best choice for the training length is shown to be larger than the number of transmit antennas and approaches half of the block length at low signal-to-jamming-and-noise ratio (SJNR). From the jammer's perspective, we derive closed-form solutions of the optimal jamming energy allocation. Numerical results demonstrate 30%–50% performance gains by using optimal designs in various scenarios. We also model the energy allocation problem as a zero-sum game and prove the existence and uniqueness of the Nash equilibrium when the training length is fixed. Furthermore, we extend our analysis to the case where the channel state information (CSI) is available at the transmitter. We show that many results found for systems with no transmitter CSI are also valid for systems with full transmitter CSI.**

***Index Terms*—Energy allocation, ergodic capacity, jamming, multiple-input–multiple-output (MIMO), nash equilibrium (NE), training-based transmission.**

I. Introduction

THE PROBLEM of jamming in wireless communications has drawn considerable attention and exists in many practical scenarios. For example, the use of jamming signals can destroy the communication of the enemy in a battlefield or result in dissatisfactory quality of service in a commercial network. Recently, jamming has also been applied on cognitive radio systems to prevent the secondary user from using the available channel [1]. Since the jammer and the legitimate user(s) of the communication channel have opposite objectives, theoretical studies often model the problem of jamming as zero-sum games [2]–[8]. The optimal transmission strategies of the transmitter and the jammer were studied in [2] from an information-theoretic viewpoint, assuming that the jammer has knowledge of the transmitted message (i.e., correlated jamming). This analysis was extended to multiple-input–multiple-output (MIMO) fading channels in [3]. Considering long-term energy constraints on blockwise transmissions, the optimal transmit and jamming energy allocations among multiple blocks were found as minimax and maximin solutions in [4] and [5]. The game-theoretical study of correlated jamming was further extended to multiple users in multiple access channels in [6] and [7], as well as multiple parallel channels in [8].

One of the main assumptions in the aforementioned works is perfect knowledge of the channel state information (CSI) at the receiver. In practical scenarios, however, the CSI needs to be estimated and, hence, is never perfectly known. One common approach to enable channel estimation at the receiver is the pilot-assisted transmission scheme (or training-based transmission scheme), in which known pilot symbols are periodically inserted into data transmission blocks [9]. When a jammer is present, jamming noise during the pilot transmission (or training) can result in poor channel estimation and hence impair the data detection. Similar to multiuser interference suppression techniques, iterative algorithms were proposed to estimate and remove jamming noises in [10] and [11]. An improved channel estimation scheme was proposed in [12] for orthogonal frequency-division multiplexing systems, which detects and removes jammed pilot subcarriers. The effect of jamming on the information capacity in wideband regime was studied in [13] and [14], and their results showed the benefit of having impulsive training that randomly changes its position in a transmission block. While the studies in [10]–[14] focused on the design from the legitimate user's point of view, very few existing results look at the design of smart jamming in training-based transmissions. Recently, jamming strategies, which make use of the legitimate user's CSI, were proposed to attack the channel estimation in singular-value-decomposition-based MIMO systems, as well as systems using space-time block codes [15].

In this paper, we study training-based MIMO systems in fading channels with jamming. In energy-constrained communications, the energy allocation between training and data transmission is an important design parameter. Many works have been devoted to analyzing the tradeoff in the transmission time and energy allocation between training and data transmission in jamming-free systems, e.g., in [16] and [17]. To the best of the authors' knowledge, no such study has been

Manuscript received October 19, 2010; revised February 23, 2011; accepted April 13, 2011. Date of publication May 10, 2011; date of current version July 18, 2011. This work was supported by the Research Council of Norway through Project 197565/V30, Project 183311/S10, and Project 176773/S10. This paper will be presented in part at the IEEE International Conference on Communications, Kyoto, Japan, June 2011. The review of this paper was coordinated by Prof. R. Schober.

X. Zhou and A. Hjørungnes are with the UNIK—University Graduate Center, University of Oslo, Kjeller, Norway (e-mail: xiangyun@unik.no; arehj@unik.no).

D. Niyato is with the School of Computer Engineering, Nanyang Technological University, Singapore 639798 (e-mail: dniyato@ntu.edu.sg).

Color versions of one or more of the figures in this paper are available online at http://ieeexplore.ieee.org.

Digital Object Identifier 10.1109/TVT.2011.2151890

carried out for systems with jamming. In this paper, we consider systems with both the legitimate user and the jammer having their own energy constraints and study the optimal energy allocation between training and data transmission, as well as the optimal training length (i.e., the number of pilot symbols in a transmission block). The figure of merit for the optimization problems is a lower bound on the ergodic capacity, which gives an achievable data rate for training-based transmission in the presence of jamming. From the legitimate user's perspective, optimizing the transmit energy allocation and training length can improve the achievable data rate. On the other hand, from the jammer's perspective, optimizing the jamming energy allocation between the training phase and the data transmission phase can degrade the data rate of the legitimate user. We provide design guidelines in various practical scenarios from the viewpoints of both the legitimate user and the jammer.

The main contributions of this work are summarized here.

1) In Section IV, we study the optimal strategy on the designer side, assuming that the opponent strategy is fixed and known to the designer. For a fixed jammer's strategy, we derive a closed-form solution for the optimal legitimate user's energy allocation and show that the optimal training length is equal to the number of transmit antennas. For a fixed legitimate user's strategy, we derive a closed-form solution for the optimal jamming energy allocation. Our results reveal that imbalance in the signal-to-jamming-and-noise ratio (SJNR) is desirable for the jammer but harmful to the legitimate user.
2) In Section V, we consider that the designer aims to find a robust (fixed) strategy that gives the best performance under the worst case scenario, assuming that the opponent can always optimize its strategy. In particular, we show that the robust choice of the training length is generally larger than the number of transmit antennas and approaches half of the block length in the low-SJNR regime.
3) In Section VI, we take a game-theoretic approach and model the energy allocation problem as a two-person zero-sum game. We prove that there always exists one and only one Nash equilibrium (NE) point when the training length is fixed.
4) We also study the case of full transmitter CSI in Section VII. We show that many results found for systems with no transmitter CSI are also valid for systems with full transmitter CSI, which can be a good message for the designer of both the legitimate user and the jammer.

The following notations will be used in this paper: Boldface upper and lower case letters denote matrices and column vectors, respectively. $\boldsymbol{I}$ is the identity matrix, $[\cdot]^\dagger$ denotes the complex conjugate transpose operation, $\mathbb{E}\{\cdot\}$ denotes the mathematical expectation, and $|\cdot|$ denotes the matrix determinant.

II. System Model

We consider a flat-fading MIMO communication system with N_t transmit antennas and N_r receive antennas, which is referred to as the legitimate user of the wireless channel. In addition, there is a jammer who aims to reduce the data rate of the legitimate user by transmitting an artificial noise signal. The received signal of the legitimate user is given by[1]

$$\boldsymbol{y} = \boldsymbol{H}\boldsymbol{x} + \boldsymbol{w} + \boldsymbol{n} \tag{1}$$

where $\boldsymbol{x}$ and $\boldsymbol{y}$ are the $N_t \times 1$ transmitted symbol vector and the $N_r \times 1$ received symbol vector, respectively. $\boldsymbol{H}$ is the $N_r \times N_t$ channel gain matrix, $\boldsymbol{w}$ is the $N_r \times 1$ received jamming noise, and $\boldsymbol{n}$ is the $N_r \times 1$ additive white Gaussian noise at the receiver. We assume that $\boldsymbol{H}$ is circularly symmetric, whose entries are independent and identically distributed (i.i.d.) zero-mean complex Gaussian random variables. The same assumption is made on $\boldsymbol{n}$ and $\boldsymbol{w}$. Although the distribution of the jamming signal $\boldsymbol{w}$ can be arbitrary in general, the Gaussian distribution is found to be the optimal choice from the jammer's design point of view for Gaussian channels in [3]. Without loss of generality, we normalize the variances of the entries in $\boldsymbol{H}$ and $\boldsymbol{n}$ to one.

A. Training-Based Transmission

We consider a training-based blockwise transmission. Each block starts with a training phase, followed by a data transmission phase. The durations of the training phase and data phase are L_p symbol periods and L_d symbol periods, respectively. Hence, the total duration of one transmission block is $L = L_p + L_d$ symbol periods. We assume that the channel gains $\boldsymbol{H}$ remain constant during one block and change to some independent values in the next block. Note that an idealized impulsive training scheme was considered in [14], in which the random positions of the pilot symbols are perfectly known to the receiver but unknown to the jammer. To realize such a scheme, the training power needs to be significantly higher than the power of the data transmission and the jamming noise, which may not be possible if the jamming power is sufficiently high. It is also unclear whether this extremely unbalanced energy allocation gives good data rate performance. In addition, the jammer may be able to confuse the receiver regarding the positions of the pilot symbols by using impulsive jamming. Therefore, we do not consider impulsive training and apply the conventional training scheme in this work.

During the training phase, the transmitter sends L_p pilot symbols, which are used by the receiver to estimate $\boldsymbol{H}$. We assume that $L_p \geq N_t$; therefore, there are at least as many measurements as unknowns for estimation. During the data transmission phase, the transmitter sends L_d data symbols, and the receiver performs coherent detection using the estimated channel gains. The signal power (per symbol) during training and data transmission is given by $\mathcal{P}_p$ and $\mathcal{P}_d$, respectively.

Apart from the legitimate user's transmission, the jammer also injects artificial noise signals. Similar to [13], we assume that the jammer knows the training-based blockwise transmission and uses different power levels to jam training and data transmission. The jamming signal power during the training phase and data phase is denoted by $\mathcal{P}_{\mathrm{wp}}$ and $\mathcal{P}_{\mathrm{wd}}$, respectively.

[1]Note that the fading gain of the channel from the jammer to the receiver is absorbed into the jamming signal $\boldsymbol{w}$ [3], [13], [14].

B. Channel Estimation

Collecting the received symbol vectors during training into an $N_r \times L_p$ matrix, we have

$$\boldsymbol{Y}_p = \boldsymbol{H}\boldsymbol{X}_p + \boldsymbol{W}_p + \boldsymbol{N}_p \tag{2}$$

where $\boldsymbol{X}_p$ is the $N_t \times L_p$ pilot matrix, and $\boldsymbol{W}_p$ and $\boldsymbol{N}_p$ are the jamming and noise matrix, respectively.

We consider the linear minimum mean square error (LMMSE) estimator [18], which is given by

$$\hat{\boldsymbol{H}} = \boldsymbol{Y}_p \left(\boldsymbol{X}_p^\dagger \boldsymbol{X}_p + (\mathcal{P}_{\mathrm{wp}} + 1)\boldsymbol{I}\right)^{-1} \boldsymbol{X}_p^\dagger \tag{3}$$

and the estimation error is given by $\tilde{\boldsymbol{H}} = \boldsymbol{H} - \hat{\boldsymbol{H}}$. The optimal $\boldsymbol{X}_p$ that minimizes the channel estimation error has an orthogonal structure such that $\boldsymbol{X}_p\boldsymbol{X}_p^\dagger = (\mathcal{P}_p L_p/N_t)\boldsymbol{I}$ [16]. With the orthogonal pilots, the variance of each element of $\tilde{\boldsymbol{H}}$ is then given by [18]

$$\sigma_{\tilde{h}}^2 = \left(1 + \frac{\mathcal{P}_p L_p}{N_t(\mathcal{P}_{\mathrm{wp}} + 1)}\right)^{-1} = \frac{\mathcal{P}_{\mathrm{wp}} + 1}{\mathcal{P}_{\mathrm{wp}} + 1 + \mathcal{P}_p L_p/N_t}. \tag{4}$$

III. Problem Formulation

We consider an energy-constrained scenario, where the total energy for a transmission block is fixed for both the legitimate user and the jammer. This can also be interpreted as a constraint on the average power over a transmission block [16]. We denote the average power budgets (i.e., variances of each element in $\boldsymbol{x}$ and $\boldsymbol{w}$) for the legitimate user and the jammer as $\mathcal{P}$ and $\mathcal{P}_w$, respectively. Indeed, $\mathcal{P}$ and $\mathcal{P}_w$ can also be seen as the average received signal power and the average received jamming power, respectively, due to the normalization in the variance of the channel gains, as well as the absorption of the jammer's channel gain into the jamming signal. We assume that the jammer has certain knowledge about the communication system that it is attacking on, including the locations of the legitimate transmitter and receiver, as well as the path-loss exponent of the wireless environment (which can be obtained through measurements). Under this assumption, the jammer can infer the values of the average received signal and jamming power, i.e., $\mathcal{P}$ and $\mathcal{P}_w$, respectively, from its measurements and the distances between the three terminals. In addition, the values of $\mathcal{P}$ and $\mathcal{P}_w$ can also be measured by the legitimate receiver and obtained at the legitimate transmitter through feedback.

In training-based transmission, an important design parameter is the energy allocation between the training phase and the data transmission phase. We denote the ratio of the total energy allocated to the training phase as ϕ and ζ for the legitimate user and the jammer, respectively. Hence, for the legitimate user, we have

$$\mathcal{P}_p = \frac{\phi \mathcal{P} L}{L_p}, \qquad \mathcal{P}_d = \frac{(1-\phi)\mathcal{P} L}{L_d}. \tag{5}$$

For the jammer, we have

$$\mathcal{P}_{\mathrm{wp}} = \frac{\zeta \mathcal{P}_w L}{L_p}, \quad \mathcal{P}_{\mathrm{wd}} = \frac{(1-\zeta)\mathcal{P}_w L}{L_d}. \tag{6}$$

Apart from the energy allocation ratio ϕ, the training length L_p (and the data length L_d) is also an important design parameter for the legitimate user.

In this paper, we provide a comprehensive study on the optimal energy allocation for both the legitimate user and the jammer in various scenarios described here.

1) *Optimal Legitimate User Design*: The jammer has a fixed jamming strategy, which can be easily measured by the legitimate user. From the legitimate user's point of view, we aim to find the optimal values of ϕ and L_p for a given value of ζ.
2) *Optimal Jammer Design*: This is the opposite case of the optimal legitimate user design, in which the roles of the legitimate user and the jammer are swapped in Scenario 1. From the jammer's point of view, we aim to find the optimal value of ζ, for the given values of ϕ and L_p.
3) *Robust Legitimate User Design*: The jammer can quickly track and react to the legitimate user's strategy, whereas the legitimate user is less capable of fast tracking and adaptation (or the legitimate user simply wants to have a fixed strategy). We describe the jammer in this scenario as a *smart* jammer. From the legitimate user's point of view, we aim to find fixed values of ϕ and L_p, which give the best performance under the worst case scenario, assuming that the smart jammer always chooses the optimal value of ζ.
4) *Robust Jammer Design*: This is the opposite case of the robust legitimate user design, in which the roles of the legitimate user and the jammer are swapped in Scenario 3. From the jammer's point of view, we aim to find a fixed value of ζ, which gives the best performance under the worst case scenario, assuming that the smart legitimate user always chooses the optimal values of ϕ and L_p.

The objective function of the aforementioned optimization problems is the achievable data rate, the supreme of which is characterized by the ergodic capacity of the legitimate user. Although the exact expression of the ergodic capacity is unknown, one commonly used lower bound can be found by following [16] and [19] as

$$C_{\mathrm{LB}} = \frac{L_d}{L}\mathbb{E}\left\{\log_2\left|\boldsymbol{I} + \rho_{\mathrm{eff}}\frac{\boldsymbol{H}_0\boldsymbol{H}_0^\dagger}{N_t}\right|\right\} \tag{7}$$

where $\boldsymbol{H}_0$ is statistically identical to $\boldsymbol{H}$, the fraction L_d/L accounts for the capacity loss due to training overhead, and ρ_{eff} is referred to as the effective signal-to-ratio (SNR) given as

$$\begin{aligned}\rho_{\mathrm{eff}} &= \frac{\left(1-\sigma_{\tilde{h}}^2\right)\mathcal{P}_d}{\mathcal{P}_{\mathrm{wd}} + 1 + \sigma_{\tilde{h}}^2\mathcal{P}_d} \\ &= \frac{\mathcal{P}_d\mathcal{P}_p L_p/N_t}{(\mathcal{P}_{\mathrm{wd}}+1)(\mathcal{P}_{\mathrm{wp}} + 1 + \mathcal{P}_p L_p/N_t) + (\mathcal{P}_{\mathrm{wp}}+1)\mathcal{P}_d}.\end{aligned} \tag{8}$$

This ergodic capacity lower bound, which gives an achievable rate, was used as the objective function to optimize the training length and energy allocation in jamming-free systems in [16], and the tightness of this bounding technique was verified for Gaussian inputs with LMMSE channel estimation in [20]. In the succeeding sections, we will use $C_{\rm LB}$ in (7) as the objective function to study the proposed optimization problems.

IV. Optimal Design Against a Fixed Opponent's Strategy

In this section, we provide analytical solutions for the *optimal legitimate user design* and the *optimal jammer design*.

A. Design of the Legitimate User

The optimal legitimate user design problem can be written as $\arg\max_{L_p,\phi} C_{\rm LB}$, and its solution is given in the following lemma:

Lemma 1: The optimal energy allocation of the legitimate user against a fixed jamming strategy (for any given training length) is given as

$$\phi^* = \begin{cases} \gamma - \sqrt{\gamma(\gamma-1)}, & \text{if } (\mathcal{P}_{\rm wp}+1)N_t > (\mathcal{P}_{\rm wd}+1)L_d \\ \frac{1}{2}, & \text{if } (\mathcal{P}_{\rm wp}+1)N_t = (\mathcal{P}_{\rm wd}+1)L_d \\ \gamma + \sqrt{\gamma(\gamma-1)}, & \text{if } (\mathcal{P}_{\rm wp}+1)N_t < (\mathcal{P}_{\rm wd}+1)L_d \end{cases} \tag{9}$$

where

$$\gamma = \frac{(\mathcal{P}_{\rm wp}+1)\mathcal{P}LN_t + (\mathcal{P}_{\rm wd}+1)(\mathcal{P}_{\rm wp}+1)L_dN_t}{(\mathcal{P}_{\rm wp}+1)\mathcal{P}LN_t - (\mathcal{P}_{\rm wd}+1)\mathcal{P}LL_d} \tag{10}$$

$$= \frac{\left(\frac{\zeta\mathcal{P}_wL}{L_p}+1\right)\mathcal{P}LN_t + \left(\frac{(1-\zeta)\mathcal{P}_wL}{L_d}+1\right)\left(\frac{\zeta\mathcal{P}_wL}{L_p}+1\right)L_dN_t}{\left(\frac{\zeta\mathcal{P}_wL}{L_p}+1\right)\mathcal{P}LN_t - \left(\frac{(1-\zeta)\mathcal{P}_wL}{L_d}+1\right)\mathcal{P}LL_d} \tag{11}$$

where (11) is obtained by substituting (6) into (10). Furthermore, the optimal training length is equal to the number of transmit antennas,[2] i.e., $L_p^* = N_t$.

Proof: See Appendix A.

The optimal energy allocation for the special case of jamming-free systems can be obtained by letting $\mathcal{P}_{\rm wp} = 0$ and $\mathcal{P}_{\rm wd} = 0$ in (9). We see from Lemma 1 that the optimal training length is the same, regardless of the presence of jamming.

The following corollary shows how ϕ^* changes with ζ.

Corollary 1: The optimal energy allocation ϕ^* is a continuous and increasing function of ζ.

Proof: See Appendix B.

Corollary 1 implies that the legitimate user should increase the training (data) power if the jammer increases its power during the training (data) phase. In other words, the legitimate user should balance the SJNR between the training and data transmission to achieve a high data rate.

In the case of $\mathcal{P}_w \gg \mathcal{P}$, i.e., the jamming power is much higher than the desired signal power, the effective SNR can be approximated as

$$\rho_{\rm eff} \approx \frac{(1-\phi)\phi(\mathcal{P}L)^2}{(\mathcal{P}_{\rm wd}+1)(\mathcal{P}_{\rm wp}+1)L_dN_t}. \tag{12}$$

[2]We presented the expression of ϕ^* for any given L_p and L_d in (9) as it will be used in later sections. With the optimal training length given by $L_p^* = N_t$, the expression of ϕ^* can be simplified by letting $L_p = N_t$ and $L_d = L - N_t$.

Hence, the optimal energy allocation strategy is given by $\phi^* = 1/2$, which is the same as the result reported in [16] for the case of asymptotically low SNR in jamming-free systems.

In the case of $\mathcal{P} \gg \mathcal{P}_w$, i.e., the desired signal power is much higher than the jamming power, the value of γ can be approximated as

$$\gamma \approx \frac{(\mathcal{P}_{\rm wp}+1)N_t}{(\mathcal{P}_{\rm wp}+1)N_t - (\mathcal{P}_{\rm wd}+1)L_d}. \tag{13}$$

We see from (13) that the optimal energy allocation strongly depends on the jamming power and the jammer's strategy, even though the desired signal is much stronger than the jamming signal. This result cannot be predicted by the high SNR analysis in jamming-free systems in [16].

B. Design of the Jammer

Now, let us turn our attention to the jammer side and study the optimal jamming energy allocation problem, which can be written as $\arg\min_\zeta C_{\rm LB}$. Since the legitimate user's strategy, i.e., ϕ and L_p, is fixed, minimizing $C_{\rm LB}$ is the same as minimizing $\rho_{\rm eff}$. Hence, the problem reduces to $\arg\min_\zeta \rho_{\rm eff}$. Intuitively, it is more efficient to jam the training phase since a short burst of strong jamming signal can effectively increase the channel estimation error and, hence, harm the data detection of the legitimate user. Therefore, one may expect that the optimal jamming strategy is to concentrate all energy in the training phase, i.e., $\zeta^* = 1$. The following lemma shows that this expectation is usually *not* correct:

Lemma 2: The optimal jamming energy allocation against a fixed legitimate user's strategy is given as

$$\zeta^* = \begin{cases} 0, & \text{if } \mathcal{P}_wL < -\kappa \\ 1, & \text{if } \mathcal{P}_wL < \kappa \\ \frac{\mathcal{P}_wL+\kappa}{2\mathcal{P}_wL}, & \text{otherwise} \end{cases} \tag{14}$$

where

$$\kappa = L_d - L_p + \mathcal{P}_dL_d - \mathcal{P}_pL_p^2/N_t \tag{15}$$

$$= L_d - L_p + \mathcal{P}L - \mathcal{P}L\phi(1+L_p/N_t) \tag{16}$$

where (16) is obtained by substituting (5) into (15).

Proof: The optimal jamming energy allocation, ζ^*, is found by solving $\arg\max_\zeta \rho_{\rm eff}^{-1}$. Substituting (6) into (8), the optimal jamming energy allocation is given by

$$\arg\max_\zeta \rho_{\rm eff}^{-1} = \arg\max_\zeta \left\{ \frac{\zeta(1-\zeta)\mathcal{P}_wL}{L_dL_p} + \frac{1-\zeta}{L_d} + \frac{\zeta}{L_p} + \frac{(1-\zeta)\mathcal{P}_pL_p}{L_dN_t} + \frac{\zeta\mathcal{P}_d}{L_p} \right\} \tag{17}$$

$$= \frac{\mathcal{P}_wL+\kappa}{2\mathcal{P}_wL} \tag{18}$$

where κ is defined in (15). Since $\zeta \in [0,1]$, ζ^* is given by (18) if it is within this range. From (17), one can show that this objective function is concave in ζ. Therefore, $\zeta^* = 1$ if (18) is greater than 1 and $\zeta^* = 0$ if (18) is smaller than 0. ■

Corollary 2: The optimal jamming energy allocation ζ^* is a continuous and non-increasing function of ϕ.

Corollary 2 implies that the jammer should increase its power during the training (data) phase if the legitimate user decreases its power during the training (data) phase. In other words, imbalance in the SJNR between the two transmission phases is desirable for the jammer.

In the case of $\mathcal{P}_w \gg \mathcal{P}$ and assuming that the jamming power is at least comparable with the receiver noise power, i.e., $\mathcal{P}_w \geq 1$, the optimal jamming energy allocation is given by

$$\zeta^* = \frac{\mathcal{P}_w L + \kappa}{2\mathcal{P}_w L} \approx \frac{\mathcal{P}_w L + L_d - L_p}{2\mathcal{P}_w L} \tag{19}$$

which is independent of the legitimate user's energy allocation strategy. In this case, it is never optimal to jam the training (or data) phase only. Furthermore, $\zeta^* = 1/2$, as $\mathcal{P}_w \to \infty$.

V. Robust Design Against the Optimal Opponent's Strategy

In this section, we investigate the problems of the *robust legitimate user design* and the *robust jammer design*.

A. Design of the Legitimate User

The robust legitimate user design problem can be written as a max-min problem: $\max_{L_p,\phi} \min_\zeta C_{\text{LB}}$. The inner (min) problem has already been solved in Section IV-B, and the optimal value of ζ is given in (14), whereas the outer (max) problem can be numerically solved. The following two lemmas provide analytical solutions in the two limiting cases of $\mathcal{P}_w \gg \mathcal{P}$ and $\mathcal{P} \gg \mathcal{P}_w$, with the assumption that the average jamming power is greater than or equal to the receiver noise power, i.e., $\mathcal{P}_w \geq 1$.

Lemma 3: In the case of $\mathcal{P}_w \gg \mathcal{P}$, the robust legitimate user design is given by

$$L_p^o = \frac{L}{2} \quad \text{and} \quad \phi^o = \frac{1}{2}. \tag{20}$$

Proof: See Appendix C.

Lemma 4: In the case of $\mathcal{P} \gg \mathcal{P}_w$, the robust legitimate user design is given by

$$L_p^o = N_t \quad \text{and} \quad \phi^o = \frac{1}{2}. \tag{21}$$

Proof: See Appendix D.

Unlike the optimal legitimate user design in which the optimal training length is always equal to the number of transmit antennas, the robust design of the training length is usually larger than the number of transmit antennas and approaches half of the block length in the low-SJNR regime.

B. Design of the Jammer

Again, we turn our attention to the jammer side and study the jamming energy allocation strategy. The problem can be written as a min-max problem: $\min_\zeta \max_{L_p,\phi} C_{\text{LB}}$. The inner (max) problem has already been solved in Section IV-A. The optimal training length is given by $L_p = N_t$, and the optimal value of ϕ is given in (9). The solution to the outer problem is stated in the following lemma for the case of $\mathcal{P}_w \geq 1$:

Lemma 5: The robust jammer design is given by

$$\zeta^o = \frac{\mathcal{P}_w L + L - 2N_t}{2\mathcal{P}_w L}. \tag{22}$$

Proof: With the optimal training length given by $L_p = N_t$, the min-max problem reduces to $\min_\zeta \max_\phi \rho_{\text{eff}}$. In Section VI, we will show that this min-max problem is equivalent to the max-min problem: $\max_\phi \min_\zeta \rho_{\text{eff}}$. In Appendix D, we have shown that the value of ϕ that solves the max-min problem with $L_p = N_t$ is given by $\phi = 1/2$. Therefore, the corresponding value of ζ, which solves the max-min (and, hence, the min-max) problem, is given by $\zeta = (\mathcal{P}_w L + \kappa)/(2\mathcal{P}_w L) = (\mathcal{P}_w L + L - 2N_t)/(2\mathcal{P}_w L)$. ■

From Lemma 5, we see that the robust jamming energy allocation depends on its power (or energy) budget. For most practical scenarios where $L > 2N_t$, ζ^o is a decreasing function of $\mathcal{P}_w$, and $\zeta^o \to 1/2$, as $\mathcal{P}_w \to \infty$.

VI. Game-Theoretic Analysis

In the previous sections, we considered the design problems from either the legitimate user side or the jammer side in various scenarios. In this section, we take a game-theoretic approach and study the behaviors of the communication system.

As the legitimate user and the jammer have exactly opposite objectives, the communication system can be modeled as a two-person zero-sum game. We consider a static game in strategic form [21]. The two players are the legitimate user and the jammer. The strategy of the legitimate user is the transmit energy allocation ϕ and the training length L_p, whereas the strategy of the jammer is the jamming energy allocation ζ. Note that the strategies are pure, as they are deterministic. The utility functions of the legitimate user and the jammer are C_{LB} and $-C_{\text{LB}}$, respectively. The main problem of interest is the existence and uniqueness of NE. For two-person zero-sum games with pure strategy spaces, NE may or may not exist, and it may not be unique if exists. When NE does exist and is reached, no player can unilaterally change its strategy to increase its utility [21].

For a two-person zero-sum game, an NE point also coincides with the max-min and min-max points [22]. The existence of an NE requires at least a max-min point and a min-max point to be co-located. From the analytical results in Section V and the numerical results to be presented in Section VIII, we know that the training length L_p at the max-min point is generally larger than N_t, whereas the training length L_p at the min-max point is always equal to N_t. In other words, the value of L_p at the max-min point is different from that at the min-max point. Therefore, NE does not exist for the game in general.

However, one can show the existence of an NE when the training length is fixed (i.e., when the training length is not part of the legitimate user's strategy in the game). This result is stated in the next lemma, which was used to prove Lemma 5 in Section V-B. Note that the utility functions of the legitimate user and the jammer reduce to ρ_{eff} and $-\rho_{\text{eff}}$, respectively, for any fixed training length.

Lemma 6: This game always has one and only one NE for any fixed training length.

Proof: The existence of NE is proven from the concavity of the utility function in the strategy of each player [22]. Recall ρ_{eff} given in (8). By substituting ϕ from (5) and directly computing the second derivative of ρ_{eff} w.r.t. ϕ, it can be shown that the second derivative is negative for any $\phi \in [0, 1]$. In addition, we have seen in the proof of Lemma 2 that ρ_{eff}^{-1} is concave in ζ. Therefore, ρ_{eff} is convex in ζ [23], which implies that $-\rho_{\text{eff}}$ is concave in ζ. The existence of NE is proven.

In Lemmas 1 and 2, we have obtained the best response of each player. Specifically, the expression of ϕ as a function of ζ, in (9), is the best response of the legitimate user, and the expression of ζ as a function of ϕ, in (14), is the best response of the jammer. Since any pair of ϕ and ζ that satisfies both (9) and (14) is an NE point, we can count the number of intersection points of the two curves described by (9) and (14) to obtain the number of NE points (see Fig. 7 for examples). Using the continuity and monotonicity results stated in Corollaries 1 and 2, one can see that there is at most one NE point. Since we have just shown the existence of NE, we conclude that there is one and only one NE point. Hence, the uniqueness is proven. ■

With the existence and uniqueness of NE, the strategy of each player is unique and known (and indeed does not need to be known) to each other before playing the game. Hence, the game always starts at the NE point, and the effective SNR or the capacity lower bound is strictly determined. For example, the strategy of the legitimate user and the jammer is given by $\phi = 1/2$ and $\zeta = (\mathcal{P}_w L + L - 2N_t)/(2\mathcal{P}_w L)$ for systems with $L_p = N_t$.

VII. Full Transmitter Channel State Information

So far, we have assumed that the transmitter has no CSI and hence uses equal power transmission among the transmit antennas. In this section, we consider the case of full transmitter CSI, which means that the transmitter has the same CSI as the receiver does. This can be achieved by having a perfect feedback link from the receiver to the transmitter, which enables the channel estimates $\hat{\boldsymbol{H}}$ to be sent back after the training phase. In reality, the feedback link is never perfect, and the imperfection can be in the form of noise or delay, which is beyond the scope of this work.

It is well known that the capacity-maximizing data transmission follows a water-filling solution. Denote the nonzero eigenvalues of $\hat{\boldsymbol{H}}^\dagger \hat{\boldsymbol{H}}$ by λ_i, where $i = 1, 2, \ldots, n$, and n is the rank of $\hat{\boldsymbol{H}}^\dagger \hat{\boldsymbol{H}}$. Following the derivation in [19], the ergodic capacity lower bound is found as

$$C_{\text{LB}} = \frac{L_d}{L}\mathbb{E}\left\{\sum_{i=1}^{n}\log_2\left(1 + \frac{1-\sigma_{\tilde{h}}^2}{\mathcal{P}_{\text{wd}} + 1 + \sigma_{\tilde{h}}^2\mathcal{P}_d}\lambda_i p_i\right)\right\} \tag{23}$$

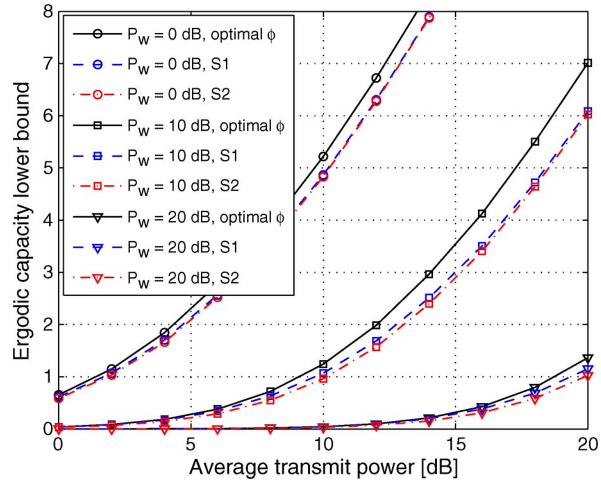

Fig. 1. Ergodic capacity lower bound C_{LB} in (7) versus the average transmit power $\mathcal{P}$ for $N_t \times N_r = 4 \times 4$ systems with a block length of $L = 50$ and training length of $L_p = 4$. The jamming energy allocation is fixed to $\zeta = 0.5$. The solid lines indicate C_{LB} achieved by using the optimal energy allocation ϕ given in (9). We also plot C_{LB} achieved by two suboptimal choices of ϕ: The dashed lines (which are denoted as S1) indicate C_{LB} achieved by using the optimal ϕ for systems in which the jamming signal is simply treated as additional receiver noise with variance of $\mathcal{P}_w$. The dash-dotted lines (which are denoted as S2) indicate C_{LB} achieved by using the optimal ϕ for jamming-free systems.

where

$$p_i = \left[\mu - \left(\frac{1-\sigma_{\tilde{h}}^2}{\mathcal{P}_{\text{wd}} + 1 + \sigma_{\tilde{h}}^2\mathcal{P}_d}\lambda_i\right)^{-1}\right]^+, \quad \sum_{i=1}^{n} p_i = \mathcal{P}_d \tag{24}$$

where $[z]^+ = \max\{0, z\}$. The following proposition summarizes a few important results in the case of full transmitter CSI.

Proposition 1: All the analytical results on the energy allocation and training length obtained for systems with no transmitter CSI, i.e., all the lemmas and corollaries in the previous sections, are also valid for systems with full transmitter CSI.

Proof: See Appendix E.

Proposition 1 implies that the optimal designs are the same for systems with no transmitter CSI and systems with full transmitter CSI in many scenarios. This is a good message for the designer of both the legitimate user and the jammer.

VIII. Numerical Results

In this section, we present numerical results for systems with no transmitter CSI to illustrate data rate improvement or degradation by using the derived energy allocation strategies.

Fig. 1 shows the legitimate user's performance gain from optimizing the energy allocation. The jammer's strategy is set to $\zeta = 0.5$, i.e., half of the total energy is used to jam the training phase. We plot C_{LB} achieved by using the optimal ϕ against jamming given in (9), as well as two suboptimal choices of ϕ for comparison, i.e., the optimal ϕ for systems in which the jamming signal is simply treated as additional receiver noise with variance of $\mathcal{P}_w$ (which is denoted as S1) and the optimal

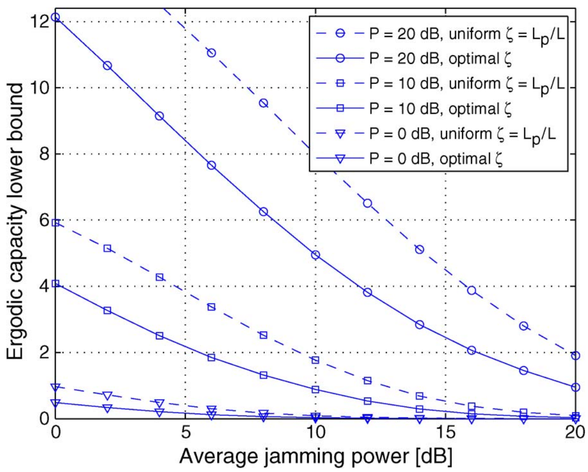

Fig. 2. Ergodic capacity lower bound $C_{\rm LB}$ in (7) versus the average jamming power $\mathcal{P}_w$ for $N_t \times N_r = 4 \times 4$ systems with a block length of $L = 50$ and a training length of $L_p = 4$. The legitimate user's energy allocation is set to the optimal ϕ for jamming-free systems. The solid lines indicate $C_{\rm LB}$ achieved by using the optimal jamming energy allocation ζ given in (14). The dashed lines indicate $C_{\rm LB}$ achieved by using the uniform jamming energy distribution $\zeta = L_p/L$.

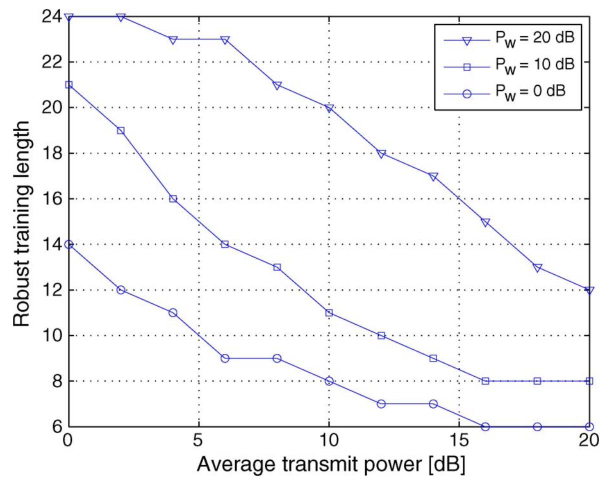

Fig. 3. Legitimate user's robust design of training length L_p^o versus the average transmit power $\mathcal{P}$ for $N_t \times N_r = 4 \times 4$ systems with a block length of $L = 50$. The jammer always chooses its optimal energy allocation strategy to minimize the ergodic capacity lower bound $C_{\rm LB}$.

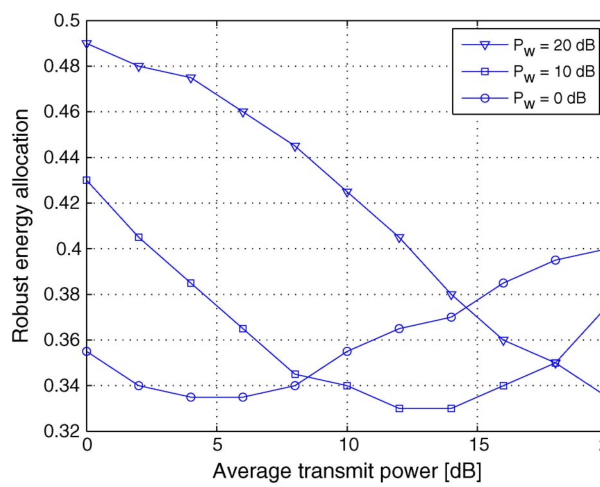

Fig. 4. Legitimate user's robust design of energy allocation ϕ^o versus the average transmit power $\mathcal{P}$ for $N_t \times N_r = 4 \times 4$ systems with a block length of $L = 50$. The jammer always chooses its optimal energy allocation strategy to minimize the ergodic capacity lower bound $C_{\rm LB}$.

ϕ for jamming-free systems (which is denoted as S2). It is clear that the data rate improvement by optimizing ϕ against jamming is significant. For example, the rate achieved using the optimal strategy, at the operating point of $\mathcal{P} = 10$ dB and $\mathcal{P}_w = 10$ dB, is 16% and 30% higher than that achieved using S1 and S2, respectively. This result clearly shows the benefit of optimizing the energy allocation according to the jammer's strategy.

Fig. 2 shows the jammer's performance gain from optimizing the energy allocation. The legitimate user's energy allocation is set to the optimal ϕ for jamming-free systems. We plot $C_{\rm LB}$ achieved by using the optimal ζ given in (14), as well as the uniform jamming energy distribution $\zeta = L_p/L$, i.e., the jamming power is fixed throughout the transmission block. It is clear that the data rate degradation by optimizing ζ is significant and can reach 50% when $\mathcal{P}_w > \mathcal{P}$.

Now, we look at the robust design of the legitimate user against smart jamming. Fig. 3 shows the robust training length L_p^o. As the average power budget $\mathcal{P}$ increases, a shorter training length is desirable for rate maximization against smart jamming. We also see that L_p^o approaches $L/2 = 25$ when $\mathcal{P} \ll \mathcal{P}_w$ and L_p^o approaches $N_t = 4$ when $\mathcal{P} \gg \mathcal{P}_w$. Note that the rate of convergence of $L_p^o \to N_t$ as $\mathcal{P}/\mathcal{P}_w \to \infty$ is slow and, hence, cannot be clearly observed in Fig. 3. For example, L_p^o reaches $N_t = 4$ at $\mathcal{P} = 30$ dB in the case of $\mathcal{P}_w = 0$ dB (plot omitted for brevity). These observations agree with our analytical results in Section V-A. Comparing the three curves with different jamming powers $\mathcal{P}_w$, one can also see that a longer training length is needed when the jamming power increases.

Fig. 4 shows the robust energy allocation ϕ^o against smart jamming. Unlike the robust training length, the value of ϕ^o is not a monotonic function of the average power budget $\mathcal{P}$. In general, we see that $\phi^o < 0.5$, i.e., more energy should be used for data transmission. We have also confirmed that ϕ^o converges to 0.5 as $\mathcal{P}/\mathcal{P}_w$ approaches zero or infinity, although the convergence as $\mathcal{P}/\mathcal{P}_w \to \infty$ is slow (plots omitted for brevity).

The performance gain of the legitimate user from using the robust design is shown in Fig. 5. First, we observe a significant rate improvement from using the robust energy allocation alone, by comparing the dashed lines with the dash-dotted lines. For example, this rate improvement at $\mathcal{P} = 10$ dB is 23% for $\mathcal{P}_w = 0$ dB and 41% for $\mathcal{P}_w = 10$ dB. Second, the additional rate improvement by using the robust training length is significant at low $\mathcal{P}$, which is observed by comparing the solid lines with the dashed lines. However, this improvement becomes less noticeable as $\mathcal{P}$ increases.

Next, we illustrate the jammer's performance gain from using the robust jamming energy allocation against a smart legitimate user in Fig. 6. Comparing with the uniform jamming energy distribution given by $\zeta = L_p/L$, the rate degradation by using the robust design is significant and can reach 30% when $\mathcal{P}_w > \mathcal{P}$.

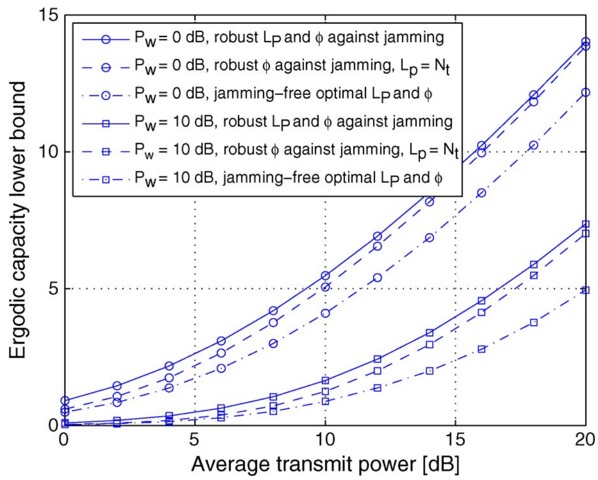

Fig. 5. Ergodic capacity lower bound $C_{\rm LB}$ in (7) versus the average transmit power $\mathcal{P}$ for $N_t \times N_r = 4 \times 4$ systems with a block length of $L = 50$. The jamming energy allocation is optimized to minimize $C_{\rm LB}$. We show $C_{\rm LB}$ achieved by using the robust design of both training length and energy allocation (solid lines), the robust design of energy allocation only (dashed lines), and the optimal design for jamming-free systems as a suboptimal choice (dash-dotted lines).

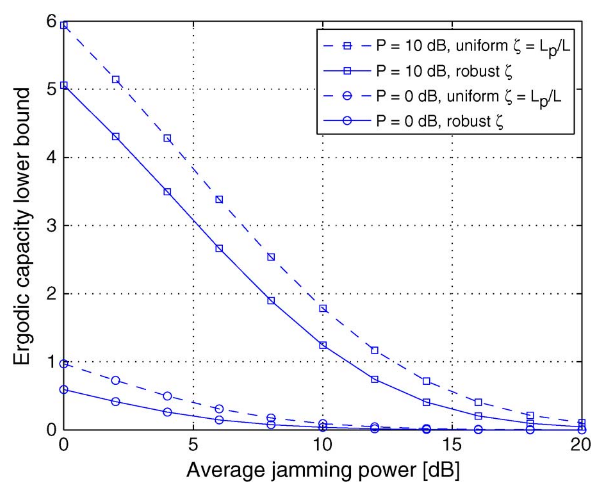

Fig. 6. Ergodic capacity lower bound $C_{\rm LB}$ in (7) versus the average jamming power $\mathcal{P}_w$ for $N_t \times N_r = 4 \times 4$ systems with a block length of $L = 50$. The legitimate user's energy allocation is optimized to maximize $C_{\rm LB}$. We show $C_{\rm LB}$ achieved by using (solid lines) the robust design of jamming energy allocation and (dashed lines) the uniform jamming energy allocation.

Finally, we take the game-theoretic view and plot the best response functions in (9) and (14) in Fig. 7 for two different scenarios. Recall that an intersection point of the best response curves corresponds to an NE point. We see from Fig. 7 that there exists exactly one NE point in both scenarios. For example, in the operating scenario of $\mathcal{P}_w = 10$ dB and $\mathcal{P} = 10$ dB, the players' strategies at the NE point are given by $\phi = 0.404$ and $\zeta = 0.428$. This result confirms the existence and uniqueness of NE proved in Lemma 6.

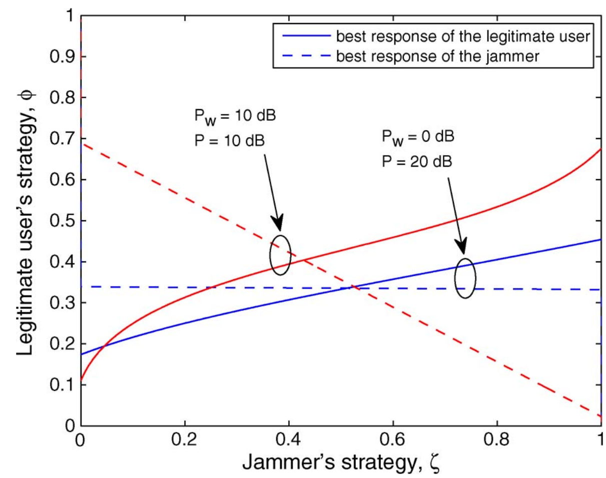

Fig. 7. Best response curves described in (9) and (14) for $N_t \times N_r = 4 \times 4$ systems with a training length of $L_p = 8$ and a block length of $L = 50$. Two operating scenarios are shown: one at $\mathcal{P}_w = 10$ dB, $\mathcal{P} = 10$ dB and the other at $\mathcal{P}_w = 0$ dB, $\mathcal{P} = 20$ dB. The intersection points of the two best response curves are the NE points.

IX. Conclusion

In this paper, we have considered a training-based MIMO system in the presence of a jammer and have studied the trade-off in energy allocation between training and data transmission. The legitimate user tries to maximize the achievable data rate by optimizing the energy allocation, as well as the training length, whereas the jammer tries to minimize the data rate of the legitimate user by optimizing the jamming energy allocation between the training phase and the data transmission phase. We have provided a comprehensive analysis in various scenarios and have derived simple design guidelines for both the legitimate user and the jammer. Our analytical results have shown to be valid for both systems with no transmitter CSI and systems with full CSI. Furthermore, we have numerically demonstrated a potential of 30%–50% performance improvement by using the optimal designs.

Appendix A
Proof of Lemma 1

We first find the optimal energy allocation, i.e., ϕ^*, for any given training length. When the training length is fixed, maximizing $C_{\rm LB}$ is the same as maximizing $\rho_{\rm eff}$. Hence, the problem reduces to $\arg\max_\phi \rho_{\rm eff}$. We follow the approach used for finding the optimal energy allocation in jamming-free systems given in [16]. Substituting (5) into (8), we have (25), shown at the bottom of the page.

If $(\mathcal{P}_{\rm wp}+1)N_t = (\mathcal{P}_{\rm wd}+1)L_d$, the optimization problem $\arg\max_\phi \rho_{\rm eff}$ reduces to

$$\arg\max_{\phi} \phi(1-\phi) = \frac{1}{2}. \tag{26}$$

$$\rho_{\rm eff} = \frac{(\mathcal{P}L)^2\phi(1-\phi)}{(\mathcal{P}_{\rm wd}+1)(\mathcal{P}_{\rm wp}+1)L_dN_t + (\mathcal{P}_{\rm wp}+1)\mathcal{P}LN_t - \left[(\mathcal{P}_{\rm wp}+1)N_t - (\mathcal{P}_{\rm wd}+1)L_d\right]\mathcal{P}L\phi}. \tag{25}$$

If $(\mathcal{P}_{\rm wp}+1)N_t > (\mathcal{P}_{\rm wd}+1)L_d$, the optimization problem $\arg\max_\phi \rho_{\rm eff}$ reduces to

$$\arg\max_{\phi} \frac{\mathcal{P}L}{(\mathcal{P}_{\rm wp}+1)N_t-(\mathcal{P}_{\rm wd}+1)L_d}\cdot\frac{\phi(1-\phi)}{\gamma-\phi} = \gamma-\sqrt{\gamma(\gamma-1)} \quad (27)$$

where γ is defined in (10) and is larger than 1 in this case.

If $(\mathcal{P}_{\rm wp}+1)N_t < (\mathcal{P}_{\rm wd}+1)L_d$, the optimization problem $\arg\max_\phi \rho_{\rm eff}$ reduces to

$$\arg\max_{\phi} -\frac{\mathcal{P}L}{(\mathcal{P}_{\rm wp}+1)N_t-(\mathcal{P}_{\rm wd}+1)L_d}\cdot\frac{\phi(1-\phi)}{\phi-\gamma} = \gamma+\sqrt{\gamma(\gamma-1)} \quad (28)$$

where γ is defined in (10) and is smaller than 0 in this case.

Next, we prove that the optimal training length is equal to the number of transmit antennas, i.e., $L_p^*=N_t$, with the optimal energy allocation previously derived. Indeed, we only need to show that $L_p^*=N_t$ *for any fixed* ϕ.

Following [16], we let σ be an arbitrary nonzero eigenvalue of $\boldsymbol{H}_0\boldsymbol{H}_0^\dagger/N_t$ and n be the rank of $\boldsymbol{H}_0\boldsymbol{H}_0^\dagger$. The ergodic capacity lower bound in (7) can be rewritten as

$$C_{\rm LB} = \frac{nL_d}{L\ln 2}\mathbb{E}\left\{\ln(1+\rho_{\rm eff}\sigma)\right\} \quad (29)$$

and its derivative w.r.t. L_d (treating L_d as a real-valued number) can be expressed as

$$\frac{dC_{\rm LB}}{dL_d} = \frac{n}{L\ln 2}\mathbb{E}\left\{\ln(1+\rho_{\rm eff}\sigma)-\frac{\rho_{\rm eff}\sigma}{1+\rho_{\rm ff}\sigma}L_d\rho_{\rm eff}\frac{d\rho_{\rm eff}^{-1}}{dL_d}\right\}. \quad (30)$$

The aim is to show that $dC_{\rm LB}/dL_d>0$ *for any fixed values* of ϕ, $\mathcal{P}_{\rm wp}$, and $\mathcal{P}_{\rm wd}$. Note that $dC_{\rm LB}/dL_d>0$ means that the optimal data (training) length takes its largest (smallest) possible value.[3] With the assumption of $L_p\ge N_t$, $dC_{\rm LB}/dL_d>0$ implies $L_p^*=N_t$.

It can be shown that $\ln(1+z)-z/(1+z)$ is an increasing function of $z\in(0,\infty)$ and it is equal to zero at $z=0$. Since $\rho_{\rm eff}\sigma\ge 0$, it can be seen that $\ln(1+\rho_{\rm eff}\sigma)-\rho_{\rm eff}\sigma/(1+\rho_{\rm eff}\sigma)\ge 0$. To show $dC_{\rm LB}/dL_d>0$, it suffices to show that $L_d\rho_{\rm eff}(d\rho_{\rm eff}^{-1}/dL_d)<1$. For any fixed ϕ, the training energy $\mathcal{P}_pL_p$ is fixed. Using (8), we have

$$L_d\rho_{\rm eff}\frac{d\rho_{\rm eff}^{-1}}{dL_d} = \frac{(\mathcal{P}_{\rm wd}+1)(\mathcal{P}_{\rm wp}+1+\mathcal{P}_pL_p/N_t)}{(\mathcal{P}_{\rm wd}+1)(\mathcal{P}_{\rm wp}+1+\mathcal{P}_pL_p/N_t)+(\mathcal{P}_{\rm wp}+1)\mathcal{P}_d} < 1. \quad (31)$$

Therefore, we have proven that $L_p^*=N_t$ *for any fixed* ϕ. This directly implies that $L_p^*=N_t$ *for the optimal value of* ϕ (which is a function of L_p). To see this, we denote the strategy of choosing ϕ and L_p as $\{\phi, L_p\}$ and denote $\phi^*(l)$ as the optimal energy allocation for $L_p=l$. Hence, we have $\{\phi^*(N_t),N_t\}1\succeq^{C_{\rm LB}}\{\phi,N_t\},\forall\phi$, where $\succeq^{C_{\rm LB}}$ is the ordering w.r.t. $C_{\rm LB}$ that the strategies give. In addition, we have just proven that $\{\phi,N_t\}\succeq^{C_{\rm LB}}\{\phi,L_p\},\forall L_p$. Combining the two ordering and choosing $\phi=\phi^*(L_p)$, we have $\{\phi^*(N_t),N_t\}\succeq^{C_{\rm LB}}\{\phi^*(L_p),L_p\},\forall L_p$. Therefore, we have proven that $L_p^*=N_t$ when *the optimal* ϕ^* is used. ■

[3] $dC_{\rm LB}/dL_d>0$ implies that $C_{\rm LB}$ increases with $L_d\in(0,\infty)$. Although, in reality, L_d only takes discrete values, $C_{\rm LB}$ still increases with $L_d\in\{1,2,3,\ldots\}$.

APPENDIX B
PROOF OF COROLLARY 1

According to (9), the range of $\zeta\in[0,1]$ is divided into (at most) three intervals in which the expression of ϕ^* has different mathematical descriptions. First, we show the continuity of ϕ^* as follows: Considering the case of $(\mathcal{P}_{\rm wp}+1)N_t>(\mathcal{P}_{\rm wd}+1)L_d$, when $(\mathcal{P}_{\rm wp}+1)N_t\to(\mathcal{P}_{\rm wd}+1)L_d$ from above, we have $\gamma\to\infty$, and hence

$$\begin{aligned}\lim_{\gamma\to\infty}\phi^* &= \lim_{\gamma\to\infty}\left\{\gamma-\sqrt{\gamma^2-\gamma}\right\}\\ &= \lim_{\gamma\to\infty}\left\{\gamma-\gamma\sqrt{1+(-\gamma)^{-1}}\right\}\\ &=\gamma-\gamma\left(1-\frac{1}{2\gamma}\right)=\frac{1}{2}\end{aligned} \quad (32)$$

where (32) is obtained using the binomial series expansion. Using a similar argument for the case of $(\mathcal{P}_{\rm wp}+1)N_t<(\mathcal{P}_{\rm wd}+1)L_d$, one can show that $\lim_{\gamma\to-\infty}\phi^*=1/2$ as $(\mathcal{P}_{\rm wp}+1)N_t\to(\mathcal{P}_{\rm wd}+1)L_d$ from below. Hence, the continuity is proven.

Next, we show that ϕ^* is an increasing function of ζ. Considering the case of $(\mathcal{P}_{\rm wp}+1)N_t>(\mathcal{P}_{\rm wd}+1)L_d$ or equivalently $\zeta>(\mathcal{P}_wL+L_d-N_t)/[\mathcal{P}_wL(1+N_t/L_p)]$, we have

$$\frac{d\phi^*}{d\gamma}=1-\frac{\gamma-\frac{1}{2}}{\sqrt{\gamma(\gamma-1)}}<1-\frac{\gamma-\frac{1}{2}}{\sqrt{\left(\gamma-\frac{1}{2}\right)\left(\gamma-\frac{1}{2}\right)}}=0. \quad (33)$$

Similarly, one can show that $d\phi^*/d\gamma<0$ for the case of $(\mathcal{P}_{\rm wp}+1)N_t<(\mathcal{P}_{\rm wd}+1)L_d$ or equivalently $\zeta<(\mathcal{P}_wL+L_d-N_t)/[\mathcal{P}_wL(1+N_t/L_p)]$. Furthermore, by taking the derivative of γ in (11) w.r.t. ζ, we find that there is no real root to $d\gamma/d\zeta=0$. This implies that γ, as a function of ζ, has neither local maximum nor local minimum. Using (11), it can also be shown that γ is continuous on $\zeta\in(-\infty,\infty)$, except for a singular point at $\zeta=(\mathcal{P}_wL+L_d-N_t)/[\mathcal{P}_wL(1+N_t/L_p)]$. When $\zeta\to(\mathcal{P}_wL+L_d-N_t)/[\mathcal{P}_wL(1+N_t/L_p)]$ from below, $\gamma\to-\infty$. When $\zeta\to(\mathcal{P}_wL+L_d-N_t)/[\mathcal{P}_wL(1+N_t/L_p)]$ from above, $\gamma\to\infty$. Therefore, γ must be a decreasing function of ζ, i.e., $d\gamma/d\zeta<0$, on both sides of the singular point. Having $d\phi^*/d\gamma<0$ and $d\gamma/d\zeta<0$, as well as the fact that ϕ^* is continuous on $\zeta\in[0,1]$, we conclude that ϕ^* is an increasing function of $\zeta\in[0,1]$. ■

APPENDIX C
PROOF OF LEMMA 3

In the case of $\mathcal{P}_w\gg\mathcal{P}$, the optimal jamming energy allocation in (14) can be approximated as

$$\zeta^*\approx\frac{\mathcal{P}_wL+L_d-L_p}{2\mathcal{P}_wL}. \quad (34)$$

Therefore, the jamming power $\mathcal{P}_{\rm wp}$ and $\mathcal{P}_{\rm wd}$ depend on the training length L_p but not on the legitimate user's energy allocation ϕ. Moreover, the effective SNR in (8) can be approximated as

$$\rho_{\rm eff} \approx \frac{(1-\phi)\phi(\mathcal{P}L)^2}{(\mathcal{P}_{\rm wd}+1)(\mathcal{P}_{\rm wp}+1)L_d N_t}. \tag{35}$$

The value of ϕ that maximizes $\rho_{\rm eff}$ is given by $\phi^o = 1/2$.

Furthermore, $\rho_{\rm eff} \to 0$ as $\mathcal{P}_w/\mathcal{P} \to \infty$, and hence, the ergodic capacity lower bound given in (29) can be approximated as

$$\begin{aligned} C_{\rm LB} &\approx \frac{nL_d}{L\ln 2}\rho_{\rm eff}\mathbb{E}\{\sigma\} & (36)\\ &\approx \frac{n\mathbb{E}\{\sigma\}}{L\ln 2}\cdot\frac{(\mathcal{P}L)^2/4}{(\mathcal{P}_{\rm wd}+1)(\mathcal{P}_{\rm wp}+1)N_t} & (37)\\ &\approx \frac{n\mathbb{E}\{\sigma\}(\mathcal{P}L)^2}{4LN_t\ln 2}\left[\left(\frac{\mathcal{P}_wL}{2(L-L_p)}+\frac{L_p}{2(L-L_p)}+\frac{1}{2}\right)\right.\\ &\qquad \left.\cdot\left(\frac{\mathcal{P}_wL}{2L_p}+\frac{L-L_p}{2L_p}+\frac{1}{2}\right)\right]^{-1} & (38)\end{aligned}$$

where (36) is obtained using Taylor's series expansion of $\ln(\cdot)$, (37) is obtained by substituting $\phi^o = 1/2$ into $\rho_{\rm eff}$ in (35), and (38) is obtained by using (34). The optimal training length is then given by

$$L_p^o = \arg\min_{L_p}\left\{\left(\frac{\mathcal{P}_wL}{2(L-L_p)}+\frac{L_p}{2(L-L_p)}+\frac{1}{2}\right)\cdot\left(\frac{\mathcal{P}_wL}{2L_p}+\frac{L-L_p}{2L_p}+\frac{1}{2}\right)\right\} \tag{39}$$

which can be directly solved to be $L/2$. ■

Appendix D
Proof of Lemma 4

We first show in the regime of $\mathcal{P} \gg \mathcal{P}_w$ that the training length for robust design is given by $L_p^o = N_t$ with the optimal jamming strategy given in (14). Recalling the proof of Lemma 1 in Appendix A, we have $dC_{\rm LB}/dL_d$ given in (30). As $\mathcal{P}/\mathcal{P}_w \to \infty$, it can be shown that $\rho_{\rm eff} = \mathcal{O}(\mathcal{P})$ and $d\rho_{\rm eff}^{-1}/dL_d = \mathcal{O}(\mathcal{P}^{-1})$, where $\mathcal{O}(\cdot)$ is the Big O notation. (The detailed derivation is tedious and straightforward and is, hence, omitted.) Therefore, $[\rho_{\rm eff}\sigma/(1+\rho_{\rm eff}\sigma)]L_d\rho_{\rm eff}(d\rho_{\rm eff}^{-1}/dL_d) = \mathcal{O}(1)$, and hence, $dC_{\rm LB}/dL_d > 0$ in the regime of $\mathcal{P} \gg \mathcal{P}_w$. This implies that the robust training length takes its smallest possible value, i.e., $L_p^o = N_t$.

Next, we prove a stronger result for the robust energy allocation. We will show that the energy allocation for robust design with $L_p = N_t$ is given by $\phi^o = 1/2$ *for any value* of $\mathcal{P}$. Substituting $L_p = N_t$ into the general expression of the effective SNR in (8), we have

$$\rho_{\rm eff} = \frac{\mathcal{P}_d\mathcal{P}_p}{(\mathcal{P}_{\rm wd}+1)(\mathcal{P}_{\rm wp}+1+\mathcal{P}_p)+(\mathcal{P}_{\rm wp}+1)\mathcal{P}_d}. \tag{40}$$

This can be rewritten in terms of ϕ and ζ using (5) and (6). The optimal jamming energy allocation given in (14) can be rewritten as

$$\zeta^* = \begin{cases} 0, & \text{if } 1 > \phi > \frac{1}{2} + \frac{\mathcal{P}_wL+L_d-L_p}{\mathcal{P}L}\\ 1, & \text{if } 0 < \phi < \frac{1}{2} - \frac{\mathcal{P}_wL-L_d+L_p}{\mathcal{P}L}\\ \frac{\mathcal{P}_wL+\kappa}{2\mathcal{P}_wL}, & \text{otherwise}\end{cases}. \tag{41}$$

Setting $\zeta = (\mathcal{P}_wL+\kappa)/(2\mathcal{P}_wL)$ and substituting it into (40), the optimal value of ϕ is found to be $\phi = 1/2$, which lies in the third case of (41), with the assumption of $\mathcal{P}_w \geq 1$. The rest is to show that there is no local optimum point in the first two cases of (41). This can be obtained using Lemma 1 and Corollary 1 as follows: When $\zeta = 0$, the optimal ϕ is smaller than 1/2; hence, no local optimum point lies in the first case of (41). When $\zeta = 1$, the optimal ϕ is larger than $1/2$; hence, no local optimum point lies in the second case of (41). Therefore, we have shown that the energy allocation for robust design is $\phi^o = 1/2$, with $L_p = N_t$. This is certainly valid for the special case of $\mathcal{P} \gg \mathcal{P}_w$. ■

Appendix E
Proof of Proposition 1

The goal is to prove that all the lemmas and corollaries obtained for systems with no transmitter CSI also hold for systems with full transmitter CSI. The proof consists of three steps as follows:

1) First, we show that the objective function for optimizing the energy allocation reduces from $C_{\rm LB}$ to $\rho_{\rm eff}$ for any *fixed training length*. From the water-filling solution of the data transmit power in (24), we can solve for the water level μ as

$$\mu = \frac{\mathcal{P}_d}{m} + \left(\frac{1-\sigma_{\tilde{h}}^2}{\mathcal{P}_{\rm wd}+1+\sigma_{\tilde{h}}^2\mathcal{P}_d}\right)^{-1}\frac{1}{m}\sum_{j=1}^{m}\lambda_j^{-1} \tag{42}$$

where m is the number of nonzero p_i in (24). Substituting μ for p_i in $C_{\rm LB}$ in (23), we have

$$C_{\rm LB} = \frac{L_d}{L}\mathbb{E}\left\{m\log_2\left(\rho_{\rm eff}+\sum_{j=1}^{m}\lambda_j^{-1}\right)+\sum_{i=1}^{m}\log_2\frac{\lambda_i}{m}\right\} \tag{43}$$

where $\rho_{\rm eff}$ is the same effective SNR, as defined in (8). For a fixed jammer's strategy, we have the following facts: Since σ_2^h and $\mathcal{P}_d$ are continuous in ϕ, we know that p_i in (24) is continuous in ϕ as well. Therefore, $C_{\rm LB}$ in (23) is also continuous in ϕ. Let us divide the range of $\phi \in [0,1]$ into subranges according to the value of m. In each subrange, the value of m is fixed, and hence, $C_{\rm LB}$ in (43) is maximized when $\rho_{\rm eff}$ reaches its maximum. At the boundaries between any two subranges, $C_{\rm LB}$ is continuous across the boundaries (since $C_{\rm LB}$ is continuous in ϕ), although m changes its value. Since $\rho_{\rm eff}$ is continuous and concave in ϕ, there is one and only one local maximum point of $\rho_{\rm eff}$ in the entire range of $\phi \in [0,1]$. This result implies that there is also one and only one local maximum point of $C_{\rm LB}$ in the entire range of $\phi \in [0,1]$. Therefore, the global maximum point of $C_{\rm LB}$

coincides with the global maximum point of $\rho_{\rm eff}$. In other words, the optimal energy allocation for the legitimate user ϕ^* is given by $\arg\max_\phi \rho_{\rm eff}$. Hence, the results on ϕ^* in Lemma 1 and Corollary 1 are obtained. Using a similar argument, one can show that the optimal jamming energy allocation ζ^* is given by $\arg\min_\zeta \rho_{\rm eff}$. Hence, the results in Lemma 2 and Corollary 2 are obtained. Having proven the results on ϕ^* in Lemma 1 and ζ^* in Lemma 2, it is seen that the NE for systems with no transmitter CSI is also the NE for systems with full transmitter CSI, for any fixed training length. Hence, Lemma 6 is obtained.

2) We prove the results regarding the optimal training length. For a fixed jammer's strategy, we need to show that the optimal training length is given by $L_p^* = N_t$ with the optimal ϕ^*. We know from Appendix A that it suffices to show $dC_{\rm LB}/dL_d > 0$ for any fixed value of ϕ, where L_d is treated as a real-valued number. In addition, it can be shown that $C_{\rm LB}$ is continuous on the read-valued variable L_d, regardless of the value of m. Therefore, it suffices to show $dC_{\rm LB}/dL_d > 0$ for any fixed values of m and ϕ. Letting $a = \sum_{j=1}^m \lambda_j^{-1}$ and $b = \sum_{i=1}^m \ln(\lambda_i/m)$, we can rewrite $C_{\rm LB}$ in (43) as

$$C_{\rm LB} = \frac{L_d}{L\ln 2}\mathbb{E}\left\{m\ln(\rho_{\rm eff}+a)+b\right\}. \tag{44}$$

The derivative of $C_{\rm LB}$ w.r.t. L_d is, hence, given by

$$\frac{dC_{\rm LB}}{dL_d} = \frac{m}{L\ln 2}\mathbb{E}\left\{\ln(\rho_{\rm eff}+a) - \frac{\rho_{\rm eff}}{\rho_{\rm eff}+a}L_d\rho_{\rm eff}\frac{d\rho_{\rm eff}^{-1}}{dL_d} + \frac{b}{m}\right\}. \tag{45}$$

From Appendix A, we know that $L_d\rho_{\rm eff}(d\rho_{\rm eff}^{-1}/dL_d) < 1$. To obtain $(dC_{\rm LB}/dL_d) > 0$, it suffices to show that

$$\ln(\rho_{\rm eff}+a) - \frac{\rho_{\rm eff}}{\rho_{\rm eff}+a} + \frac{b}{m} \geq 0 \tag{46}$$

which is an increasing function in $\rho_{\rm eff}$. Hence, it suffices to show the preceding inequality with $\rho_{\rm eff} = 0$, i.e.,

$$\begin{aligned}\ln a + \frac{b}{m} &= \ln\sum_{j=1}^m \lambda_j^{-1} + \frac{1}{m}\sum_{i=1}^m \ln\frac{\lambda_i}{m}\\ &\geq \frac{1}{m}\sum_{j=1}^m \ln\left(\frac{\lambda_j}{m}\right)^{-1} + \frac{1}{m}\sum_{i=1}^m \ln\frac{\lambda_i}{m} = 0\end{aligned} \tag{47}$$

where we have used the concavity of $\ln(\cdot)$ to obtain (47). Therefore, the optimal training length L_p^* in Lemma 1 is obtained. Using the results obtained so far, it is not difficult to prove Lemma 5 as well.

3) We obtain the result on the robust energy allocation and training length for the legitimate user in the cases of $\mathcal{P}_w \gg \mathcal{P}$ and $\mathcal{P} \gg \mathcal{P}_w$. When $\mathcal{P}_w \gg \mathcal{P}$, the water-filling solution is given by putting all transmit power into the strongest eigenchannel, i.e., $p_1 = \mathcal{P}_d$ with λ_1 being the largest eigenvalue. The ergodic capacity lower bound in (23) reduces to

$$C_{\rm LB} = \frac{L_d}{L}\mathbb{E}\left\{\log_2(1+\rho_{\rm eff}\lambda_1)\right\}. \tag{48}$$

Lemma 3 can then be proven by following the derivation in Appendix C. When $\mathcal{P} \gg \mathcal{P}_w$, the water-filling solution reduces to the equal power allocation used in systems with no transmit CSI; hence, Lemma 4 is obtained as well. We have now proven all the lemmas and corollaries. ■

REFERENCES

[1] R. Chen, J.-M. Park, and K. Bian, "Defense against primary user emulation attacks in cognitive radio networks," *IEEE J. Sel. Areas Commun.*, vol. 26, no. 1, pp. 25–37, Jan. 2008.

[2] M. Médard, "Capacity of correlated jamming channels," in *Proc. 35th Allerton Conf. Commun., Control Comput.*, vol. 1997, pp. 1043–1052.

[3] A. Kashyap, T. Basar, and R. Srikant, "Correlated jamming on MIMO Gaussian fading channels," *IEEE Trans. Inf. Theory*, vol. 50, no. 9, pp. 2119–2123, Sep. 2004.

[4] G. T. Amariucai, S. Wei, and R. Kannan, "Minimax and maxmin solutions to Gaussian jamming in block-fading channels under long term power constraints," in *Proc. 41st Annu. CISS*, Baltimore, MD, Mar. 2007, pp. 312–317.

[5] G. T. Amariucai, S. Wei, and R. Kannan, "Gaussian jamming in block-fading channels under long term power constraints," in *Proc. IEEE ISIT*, Nice, France, Jun. 2007, pp. 1001–1005.

[6] S. Farahmand, G. B. Giannakis, and X. Wang, "Max-min strategies for power-limited games in the presence of correlated jamming," in *Proc. 41st Annu. CISS*, Baltimore, MD, Mar. 2007, pp. 300–305.

[7] S. Shafiee and S. Ulukus, "Mutual information games in multiuser channels with correlated jamming," *IEEE Trans. Inf. Theory*, vol. 55, no. 10, pp. 4598–4607, Oct. 2009.

[8] R. H. Gohary, Y. Huang, Z.-Q. Luo, and J.-S. Pang, "A generalized iterative water-filling algorithm for distributed power control in the presence of a jammer," in *Proc. IEEE ICASSP*, Taipei, Taiwan, Apr. 2009, pp. 2373–2376.

[9] J. K. Cavers, "An analysis of pilot symbol assisted modulation for Rayleigh fading channels," *IEEE Trans. Veh. Technol.*, vol. 40, no. 4, pp. 686–693, Nov. 1991.

[10] H. El Gamal and E. Geraniotis, "Iterative channel estimation and decoding for convolutionally coded anti-jam FH signals," *IEEE Trans. Commun.*, vol. 50, no. 2, pp. 321–331, Feb. 2002.

[11] J.-W. Moon, T. F. Wong, and J. M. Shea, "Pilot-assisted and blind joint data detection and channel estimation in partial-time jamming," *IEEE Trans. Commun.*, vol. 54, no. 11, pp. 2092–2102, Nov. 2006.

[12] M. Han, T. Yu, J. Kim, K. Kwak, S. Lee, S. Han, and D. Hong, "OFDM channel estimation with jammed pilot detector under narrow-band jamming," *IEEE Trans. Veh. Technol.*, vol. 57, no. 3, pp. 1934–1939, May 2008.

[13] S. Ray, P. Moulin, and M. Médard, "On optimal signaling and jamming strategies in wideband fading channels," in *Proc. IEEE Workshop SPAWC*, Cannes, France, Jul. 2006, pp. 1–5.

[14] S. Ray, P. Moulin, and M. Médard, "On jamming in the wideband regime," in *Proc. IEEE ISIT*, Seattle, WA, Jul. 2006, pp. 2574–2577.

[15] R. Miller and W. Trappe, "Subverting MIMO wireless systems by jamming the channel estimation procedure," in *Proc. ACM Conf. WiSec*, 2010, pp. 19–24.

[16] B. Hassibi and B. M. Hochwald, "How much training is needed in multiple-antenna wireless links?" *IEEE Trans. Inf. Theory*, vol. 49, no. 4, pp. 951–963, Apr. 2003.

[17] V. Pohl, P. H. Nguyen, V. Jungnickel, and C. Helmolt, "Continuous flat-fading MIMO channels: Achievable rate and optimal length of the training and data phases," *IEEE Trans. Wireless Commun.*, vol. 4, no. 4, pp. 1889–1900, Jul. 2005.

[18] S. M. Kay, *Fundamentals of Statistical Signal Processing: Estimation Theory*. Englewood Cliffs, NJ: Prentice-Hall, 1993.

[19] T. Yoo and A. Goldsmith, "Capacity and power allocation for fading MIMO channels with channel estimation error," *IEEE Trans. Inf. Theory*, vol. 52, no. 5, pp. 2203–2214, May 2006.

[20] X. Zhou, P. Sadeghi, T. A. Lamahewa, and S. Durrani, "Design guidelines for training-based MIMO systems with feedback," *IEEE Trans. Signal Process.*, vol. 57, no. 10, pp. 4014–4026, Oct. 2009.

[21] M. Felegyhazi and J.-P. Hubaux, "Game theory in wireless networks: A tutorial," EPFL, Lausanne, Switzerland, Tech. Rep. LCA-REPORT-2006-002, 2006.

[22] E. B. Yanovskaya, "Infinite zero-sum two-person games," *J. Sov. Math.*, vol. 2, pp. 520–541, May 1974.
[23] S. Boyd and L. Vandenberghe, *Convex Optimization,* 1st ed. Cambridge, U.K.: Cambridge Univ. Press, 2004.

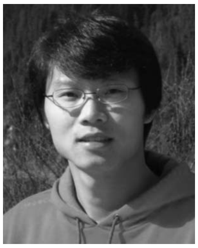

Xiangyun Zhou (S'08–M'11) received the B.E. (Hons.) degree in electronics and telecommunications engineering and the Ph.D. degree in telecommunications engineering from the Australian National University, Canberra, Australia, in 2007 and 2010, respectively.

He is currently a Postdoctoral Research Fellow with UNIK—University Graduate Center University of Oslo, Kjeller, Norway. His research interests are wireless communications and signal processing, including multiple-input–multiple-output systems, ad hoc networks, relay and cooperative communications, and physical-layer security.

Dusit Niyato (M'09) received the B.E. degree from King Mongkut's Institute of Technology Ladkrabang, Bangkok, Thailand, in 1999 and the Ph.D. degree in electrical and computer engineering from the University of Manitoba, Winnipeg, MB, Canada, in 2008.

He is currently an Assistant Professor with the Division of Computer Communications, School of Computer Engineering, Nanyang Technological University, Singapore. His current research interests include the design, analysis, and optimization of wireless communication, smart grid systems, green radio communications, and mobile cloud computing.

Are Hjørungnes (SM'06) received the M.Sc. degree (with honors) from Norwegian Institute of Technology, Trondheim, Norway, in 1995 and the Ph.D. degree from the Norwegian University of Science and Technology, Trondheim, in 2000.

He was a Professor with the Faculty of Mathematics and Natural Sciences, UNIK—University Graduate Center (UNIK), University of Oslo, Kjeller, Norway. From August 2000 to December 2000, he was a Researcher with the Tampere International Center for Signal Processing, Tampere University of Technology, Tampere, Finland. From March 2001 to July 2002, he was a Postdoctoral Fellow with the Signal Processing Laboratory, Federal University of Rio de Janeiro, Rio de Janeiro, Brazil. From September 2002 to August 2003, he was a Postdoctoral Fellow with the Signal Processing Laboratory, Helsinki University of Technology, Helsinki, Finland. From September 2003 to August 2004, he was a Postdoctoral Fellow with the Digital Signal Processing and Image Analysis Group, Department of Informatics, University of Oslo. He has held visiting appointments with the Image and Signal Processing Laboratory, University of California, Santa Barbara; the Signal Processing Laboratory, Federal University of Rio de Janeiro; the Mobile Communications Department, Eurecom Institute, Valbonne, France; the University of Manitoba, Winnipeg, MB, Canada; the Alcatel-Lucent Chair at SUPÉLEC, France; the Department of Electrical and Computer Engineering, University of Houston, TX; the Department of Electrical and Computer Engineering, University of California, San Diego; and the Department of Electrical Engineering, University of Hawaii, Manoa. He authored the book *Complex-Valued Matrix Derivatives: With Applications in Signal Processing and Communications* (Cambridge University Press, 2011). His current research interests are signal processing, communications, and wireless networks.

Prof. Hjørungnes has been serving as an Editor for the IEEE TRANSACTIONS ON WIRELESS COMMUNICATIONS since March 2007. In 2010 and 2011, he was a Guest Editor for the IEEE JOURNAL OF SELECTED TOPICS IN SIGNAL PROCESSING and the IEEE JOURNAL ON SELECTED AREAS IN COMMUNICATIONS for the Special Issues on "Model Order Selection in Signal Processing Systems" and "Cooperative Networking—Challenges and Applications." He was the recipient of Best Paper Awards at the IEEE International Conference on Wireless Communications, Networking, and Mobile Computing; the 7th International Symposium on Modeling and Optimization in Mobile, Ad Hoc, and Wireless Networks; and the 5th International Conference on Internet Monitoring and Protection.